

LETTER • OPEN ACCESS

Substantial carbon sequestration by peatlands in temperate areas revealed by InSAR

To cite this article: Behshid Khodaei *et al* 2023 *Environ. Res. Lett.* **18** 044012

View the [article online](#) for updates and enhancements.

You may also like

- [Impacts of 25 years of groundwater extraction on subsidence in the Mekong delta, Vietnam](#)
P S J Minderhoud, G Erkens, V H Pham et al.
- [Assessment of hydrologic connectivity in an ungauged wetland with InSAR observations](#)
Fernando Jaramillo, Ian Brown, Pascal Castellazzi et al.
- [Atmospheric phase delay correction of PS-InSAR to Monitor Land Subsidence in Surabaya](#)
Toifatul Ulma, Ira Mutiara Anjasmara and Noorlaila Hayati

ENVIRONMENTAL RESEARCH
LETTERS

LETTER

Substantial carbon sequestration by peatlands in temperate areas revealed by InSAR

OPEN ACCESS

RECEIVED

24 February 2022

REVISED

2 February 2023

ACCEPTED FOR PUBLICATION

6 March 2023

PUBLISHED

21 March 2023

Original content from this work may be used under the terms of the [Creative Commons Attribution 4.0 licence](#).

Any further distribution of this work must maintain attribution to the author(s) and the title of the work, journal citation and DOI.

Behshid Khodaei^{1,2,*} , Hossein Hashemi^{1,2} , Shokoufeh Salimi³ and Ronny Berndtsson^{1,2}¹ Division of Water Resources Engineering, Lund University, Lund, Sweden² Centre for Advanced Middle Eastern Studies, Lund University, Lund, Sweden³ Department of Forest Ecology and Management, Swedish University of Agricultural Sciences, Umeå, Sweden

* Author to whom any correspondence should be addressed.

E-mail: behshid.khodaei@tvr.lth.se**Keywords:** InSAR, peatland, carbon sequestration, deformation, SwedenSupplementary material for this article is available [online](#)**Abstract**

Peatlands are unique ecosystems that contain massive amounts of carbon. These ecosystems are incredibly vulnerable to human disturbance and climate change. This may cause the peatland carbon sink to shift to a carbon source. A change in the carbon storage of peatlands may result in surface deformation. This research uses the interferometric synthetic aperture radar (InSAR) technique to measure the deformation of the peatland's surface in south Sweden in response to the seasonal and extreme weather conditions in recent years, including the unprecedented severe drought in the summer of 2018. The deformation map of the study area is generated through a time-series analysis of InSAR from June 2017 to November 2020. Monitoring the peatland areas in this region is very important as agricultural and human activities have already caused many peatlands to disappear. This further emphasizes the importance of preserving the remaining peat sites in this region. Based on the InSAR results, a method for calculating the carbon flux of the peat areas is proposed, which can be utilized as a regular monitoring approach for other remote areas. Despite the severe drought in the summer of 2018, our findings reveal a significant uplift in most of the investigated peat areas during the study period. Based on our estimations, 86% of the peatlands in the study area experienced an uplift corresponding to about 47 000 tons of carbon uptake per year. In comparison, the remaining 14% showed either subsidence or stable conditions corresponding to about 2300 tons of carbon emission per year during the study period. This emphasizes the importance of InSAR as an efficient and accurate technique to monitor the deformation rate of peatlands, which have a vital role in the global carbon cycle.

1. Introduction

Wetlands are among the most productive ecosystems on earth, representing an essential role in water supply and purification, carbon sequestration, and climate change mitigation (Campbell *et al* 2009, Wdowinski and Hong 2015). Peatlands are a particular type of natural wetlands distinguished by peat accumulation (i.e. incomplete decayed vegetation) (Dunn and Freeman 2011, Salimi *et al* 2021a). The peatlands are unique ecosystems that contain a massive amount of carbon. Most peatland areas (about 80%) can be found in temperate-cold climates in the northern hemisphere, widespread in the boreal and subarctic zones (Premke *et al* 2016). Although peatlands only

cover 3%–4% of the global land area, they contain approximately 25% of global soil carbon (Gorham *et al* 1991), demonstrating their significance in carbon cycle dynamics (Dise 2009). Peatlands provide many ecosystem services, such as climate regulation, water purification, biodiversity, and flood control. There is a risk that these services will become disservices due to human disturbance and climate change (Salimi *et al* 2021a, 2021b). Sweden is a peat-rich country, with more than 15% of its land area covered by peatlands that significantly contribute to the worldwide carbon cycle.

Disruption of the hydrological balance in a peatland due to water table changes leads to accumulation or degradation of organic matter, observed as

peat surface uplift or subsidence, respectively (Fritz *et al* 2008, Potvin *et al* 2015). In other words, there is a close relationship between the water table depth in a peatland and its general state (Potvin *et al* 2015). Changes in the water table due to different natural or manmade activities can affect the peat conditions and, consequently, its carbon sequestration capabilities (Alshammari *et al* 2018). For example, water table decline in peat areas may speed up the decomposition process, manifesting itself as subsidence and leading to the release of greenhouse gases (i.e. CO₂, CH₄, N₂O) into the atmosphere and nutrient release into receiving water bodies (Lundblad 2015, Salimi *et al* 2021a). Lund *et al* (2012) investigated the effect of drought periods on southern Sweden's temperate nutrient-poor peat area. They found that the drought's timing, severity, and duration affect peatland respiration and net ecosystem exchange.

Several studies have related the amount of carbon exchange between peat areas and the atmosphere to the volumetric change in those areas (Fritz *et al* 2008, Hooijer *et al* 2012, Couwenberg and Hooijer 2013). The uplift or subsidence of the peat area surface is correlated with the peat accumulation or loss, respectively (Hooijer *et al* 2012). The artificial or natural change of the water table in the peat area is considered a leading cause of peat surface deformation (Price 2003, Holden *et al* 2004). Hence, monitoring the peat surface deformation can provide valuable insights into the peat condition and its contribution to the carbon cycle, including uplift caused by the accumulation of organic matter (Large *et al* 2021) and irreversible or reversible subsidence due to water drainage and degradation of organic matter.

Vertical deformation of sparse points on the earth's surface can be accurately measured using the height leveling technique and Global Positioning Systems discretely and continuously over time (Reeve *et al* 2013). However, high cost and spatiotemporal gaps between discrete measurements cause reduced efficiency, especially in the time-series (TS) analysis of peat surface deformation. Moreover, difficulties in accessing remote areas, especially peatlands, limit potential observations. The interferometric synthetic aperture radar (InSAR) technique has gained attention as an alternative approach to monitoring the earth's surface deformation over time and space with sub-centimeter precision. The TS-InSAR is used to monitor seasonal and long-term deformation of the earth's surface over a specified time interval (Chen *et al* 2000, 2016, Reeves *et al* 2014, Smith *et al* 2021).

Several studies have utilized InSAR in assessing the conditions of wetlands (e.g. Xie *et al* 2013, Wdowinski and Hong 2015, Jaramillo *et al* 2018, Mohammadimanesh *et al* 2018) and peatlands (e.g. Zhou 2013, Cigna *et al* 2014, Alshammari *et al* 2018, Marshall *et al* 2018, 2022, Zhou *et al* 2019, Amani *et al* 2021, Umarhadi *et al* 2021). Alshammari *et al* (2020)

applied the TS-InSAR technique to classify peat surface conditions based on seasonal and long-term deformation rates of the peat's surface but without providing a link to carbon flux. Hoyt *et al* (2020) used InSAR combined with peat material properties to estimate the CO₂ emissions over tropical peatlands of Southeast Asia and connected their findings to sites with considerable degradation and change in water table levels.

Sweden is one of the most peat-rich countries globally. Peatlands make up 15.2% of its territory (Lundblad 2015). As climate change is likely to impact peatland ecosystems in the near future (Franzén 2006), Salimi *et al* (2021b) studied the impact of the 2018 drought (i.e. current scenario) as well as future climate scenarios on peat areas in an experiment within climate control chambers. They discovered that the peat under the current climate and slightly warmer climate scenario could maintain their sink function during the drought, i.e. 2018, and benefit from the growing season, i.e. 2019, with a higher rate of CO₂ uptake. However, they emphasized that this would not be the case for the warmer climate scenarios, where plants would experience higher drought stress leading to the loss of their photosynthetic capability and CO₂ sink function. Unfortunately, there is a substantial lack of high-quality observations regarding peatland conditions in southern Sweden. Existing observations do not reflect the current peatland situation and are not updated regularly. This makes it challenging to evaluate the effects of climate change.

For this purpose, we investigated the peat surface deformation and its contribution to the carbon cycle for a major part of Skåne county in southern Sweden over three years, from June 2017 to November 2020, using high-resolution InSAR data. The novelty of this study lies partly in the improved understanding of peatland response to dry heat spells in a temperate environment (Hedwall and Brunet 2016) and also partly in the implemented InSAR method to measure these processes and provide up-to-date and continuous insight into the current conditions of peatland in the study area. The presented observations support extensive lab and field experiments performed during 2017–2020, when substantial uplift in the peat surfaces after the severe drought in summer of 2018 was observed. Estimation of the carbon sequestration is derived by considering the contribution of local peatlands. To the best of the authors' knowledge, this work is the first study that has utilized the high-precision InSAR monitoring method in peatland areas specific to southern Sweden, validated with extensive laboratory measurements.

2. Study area and data

Skåne county is Sweden's southernmost province, with an estimated area of 11 000 km² surrounded by

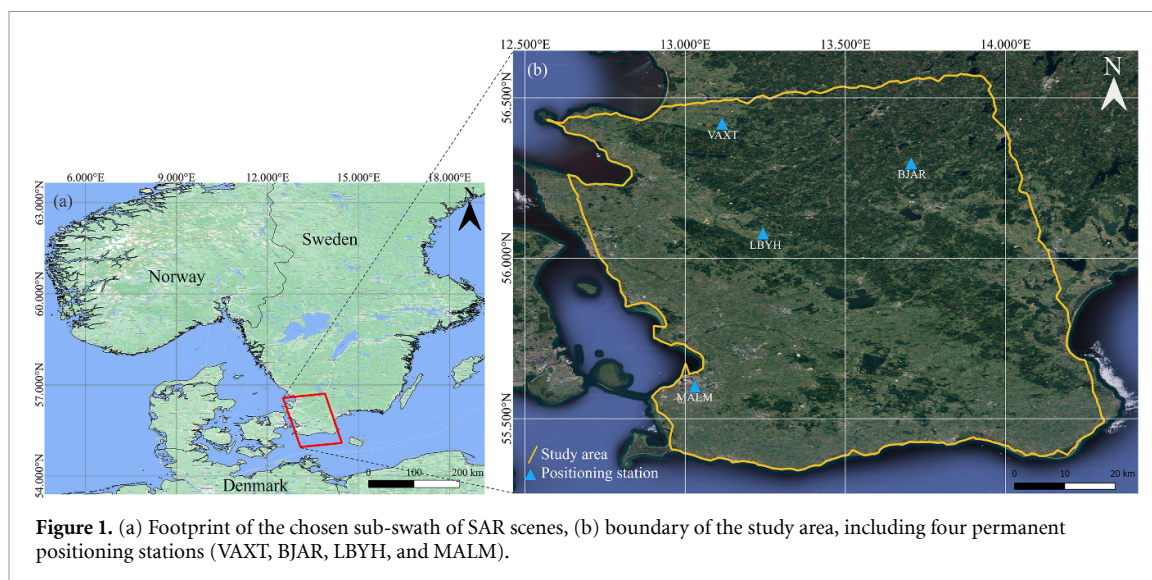


Figure 1. (a) Footprint of the chosen sub-swath of SAR scenes, (b) boundary of the study area, including four permanent positioning stations (VAXT, BJAR, LBYH, and MALM).

water in the west, east, and south. It is often considered the chief food producer of the country as a large part of the land in this region is used for agricultural purposes. The region has various land use types, including expanding urban and industrial zones, arable land, forests, wetlands, and water bodies (Official Statistics of Sweden 2020). In Skåne, 9% of the land area is covered by organic soil, including peat layers (Lundblad 2015). Skåne is the only province in Sweden located in the temperate region, unlike the rest of the country's boreal, subarctic, and Arctic climates. Although this province has less peatland coverage than the rest, there is a concern for the peatlands in this temperate zone due to intensive human disturbance. Concerns for this region will grow as the adverse effects of climate change on these disturbed peatlands become more severe, leading to decreased ability to sequester carbon in the future (Salimi *et al* 2021b).

In selecting the specific study area, the western VV-polarization sub-swath from a set of 101 Interferometric Wide Swath Level-1 Sentinel-1B images in ascending track number 73 was chosen, covering two-thirds of all peatlands of Skåne. The study period covered 42 months, from June 2017 to November 2020. Daily measurement data from four permanent positioning stations were used to validate the InSAR processing. Figure 1(a) shows the footprint of the chosen sub-swath of selected SAR scenes on a geographic map, and figure 1(b) shows the boundary of the study area and the location of four permanent positioning stations named MALM (Malmö), BJAR (Bjärnum), VAXT (Våxtorp), and LBYH (Ljungbyhed).

The boundary map of the wetlands, including peatlands in the study area, was provided by Sweden's National Wetlands Inventory (VMI), which has been responsible for wetland surveying in Sweden since the mid-1980s (Gunnarsson and Löfroth 2014). Amongst

the 1239 wetland sites in Skåne, 834 sites (i.e. 67%) were covered by the selected sub-swath of Sentinel-1 images in this study (figure S1(c)).

VMI distinguishes peatlands as a sub-category of wetlands that have the capacity to accumulate peat. VMI has two distinct classifications for the mapped wetlands. The first classification includes four classes (I, II, III, IV) based on their importance in representativity, size, intactness, diversity, and rarity. A lower class number corresponds to a higher nature conservation and environmental value of the site based on VMI's interpretation. In other words, class I has the highest nature conservation and ecological value, and class IV has the lowest. In the second classification, the sites were categorized using remote sensing and field surveys based on their vegetation type (Sjörs 1967). These include bogs (eccentric, concentric, and raised bog), fens, and mixed types. The purpose of using the abovementioned classification in this study was to improve the understanding of the conditions of detected sites in terms of dominant vegetation species as well as their preservation priority.

3. Methodology

As the study region is highly vegetated, a short baseline subset-based InSAR technique implemented in the Stanford Method for Persistent Scatterers (StaMPS)/multi-temporal InSAR (MTI) as an extended version of StaMPS package was used for measuring deformation over the study area (Ferretti *et al* 2000, Berardino *et al* 2002, Hooper *et al* 2004, 2007, Hooper 2008, Tong and Schmidt 2016). A set of 369 multiple small baseline interferograms was formed between images by considering threshold values for perpendicular and temporal baselines equal 150 m and 60 days, respectively. The criteria here was that the resulting interferograms have a strong connection

with each other such that the deformation can be continuously tracked in time through a short baseline network of interferograms (see section 1 of supplementary material). The StaMPS/MTI method uses the full resolution images to identify pixels with a low decorrelation rate over time, named slowly decorrelating filtered phase (SDFP), using the considered network of interferograms (figure S1(a)). The StaMPS/MTI processing output includes long-term deformation rate and TS deformation of the detected SDFP pixels in the satellite line of sight (LOS) direction. The deformation rate was projected in the vertical direction, assuming its horizontal component is negligible, which was the case for the available positioning stations distributed over the area. The vertical deformation rate is derived as follows:

$$D_v = \frac{D_{LOS}}{\cos(\theta_i)} \quad (1)$$

where D_v and D_{LOS} are deformation rates in vertical and LOS direction, respectively, and θ_i is the look angle for each SDFP pixel. Detailed information about the used InSAR method is presented in the supplementary material. The accuracy of the deformation data was evaluated using the root mean square error (RMSE) calculation between the TS-InSAR data against positioning stations' data (section 2 of supplementary material).

Next, peat sites were selected where a minimum number of five SDFP pixels fell within their territories, with at least one SDFP pixel in every 100 ha. The mean deformation rate of each site over time was calculated by averaging the deformation rate of all detected SDFP pixels.

The CO_2 flux of peat soil can be calculated using equation (2) based on the volumetric change in accumulated peat volume (Hoyt et al 2020) as:

$$C_{em/ab} = A \times D_v \times BD \times C_{org} \quad (2)$$

where $C_{em/ab}$ is the amount of carbon emitted or absorbed by the peat site ($kg\ yr^{-1}$), A is the area of the peat site (m^2), D_v is the average deformation rate of all SDFP pixels inside each site ($m\ yr^{-1}$), BD is the dry bulk density of the peat ($kg\ m^{-3}$), and C_{org} is the organic carbon content (unitless). The dry bulk density and carbon content were assumed to be $0.08\ g\ cm^{-3}$ and 0.55, respectively, based on suggested values in similar studies (Couwenberg and Hooijer 2013, Liu and Lennartz 2019, Hoyt et al 2020). The dry bulk density was estimated at $0.08\ g\ cm^{-3}$ for tropical (Hoyt et al 2020) and boreal (Liu and Lennartz 2019) peat sites. Our study area is mainly considered a temperate climate, a transition between tropical and boreal. Thus, it is reasonable to consider $0.08\ g\ cm^{-3}$ for dry bulk density. Based on the sign of the D_v , the calculated $C_{em/ab}$ can be regarded as the peat site emission or absorption of carbon.

4. Results and discussion

4.1. Deformation analysis

The long-term deformation rates of SDFP pixels over the study area were calculated using the InSAR technique during the 2017–2020 period (figure S1(b)).

Regarding validation of InSAR, the RMSE between TS data of each of the four permanent positioning stations and all detected SDFP pixels within a circle of $r = 100\ m$ around each station was calculated to range between 4 and 8 mm. Furthermore, the absolute difference between the deformation rate based on the data from each positioning station and the InSAR processing results ranged between 0.2 and $1.4\ mm\ yr^{-1}$. As these errors are within the positioning stations' uncertainty, the InSAR processing validity can be confirmed. InSAR validation is discussed in detail in section 2 of the supplementary material.

The InSAR deformation map was used to select the peat sites that play a role in carbon flux in the study area based on the criteria discussed in section 3 (figure S1(b)). This resulted in 64 different sites that could be classified in three ways, as shown in figure 2. Three types of classifications are shown in this figure. Two classifications (figures 2(a) and (b)) are based on the VMI maps discussed in the study area section. Figure 2(a) shows eight different types of peatlands, including four bog types (eccentric, concentric, raised, and indeterminable) and four mixed types (table S2). Notably, all mixed-type sites also include bogs, and the detected SDFP pixels were primarily located in the areas containing bogs. Figure 2(b) shows the classification based on their nature conservation and environmental value (table S3). Figure 2(c) depicts the classification of the deformation rate of the detected sites, that is the output of the InSAR processing, which led to the identification of three groups, i.e. sites with uplift, subsidence, or stable sites, based on the mean long-term deformation rate of the detected SDFP pixels inside each site (table S4). Stable sites were defined as sites having an absolute deformation rate of less than a certain threshold. The threshold was defined as the average of the abovementioned RMSE for the four permanent stations normalized by the study duration.

Figure 3 summarizes the results of this study in a quantitative manner. According to figure 3(a), class I, II, and III occupied 17%, 50%, and 22% of all 64 detected sites, respectively. Only seven remaining sites (11%), which were all raised bog type, fell into class IV (table S3). From 64 detected sites, 54 sites (84%) were classified as bog type, including concentric, eccentric, raised, mixed, and indeterminable bogs. For the remaining ten sites, eight sites (13% of total sites) were categorized as mixed fen, and the other two (3% of total sites) were categorized as mixed wetlands (table S2).

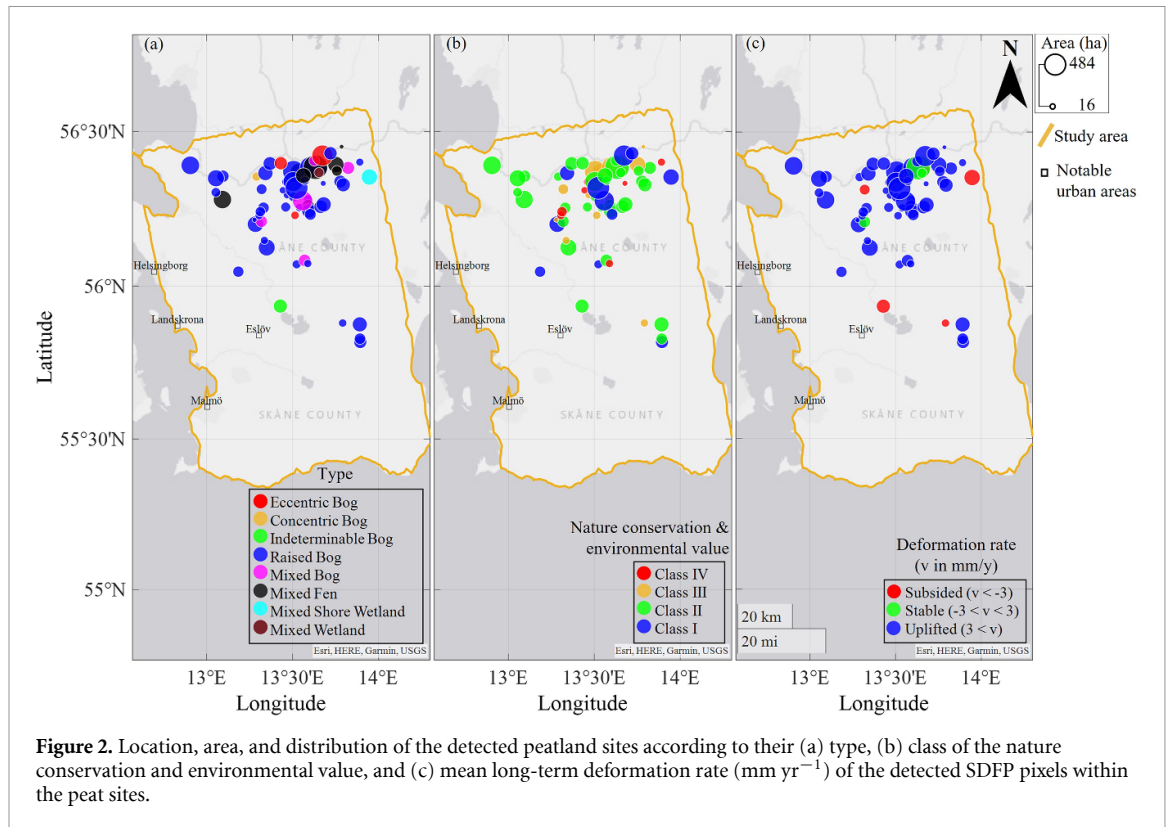


Figure 2. Location, area, and distribution of the detected peatland sites according to their (a) type, (b) class of the nature conservation and environmental value, and (c) mean long-term deformation rate (mm yr^{-1}) of the detected SDFP pixels within the peat sites.

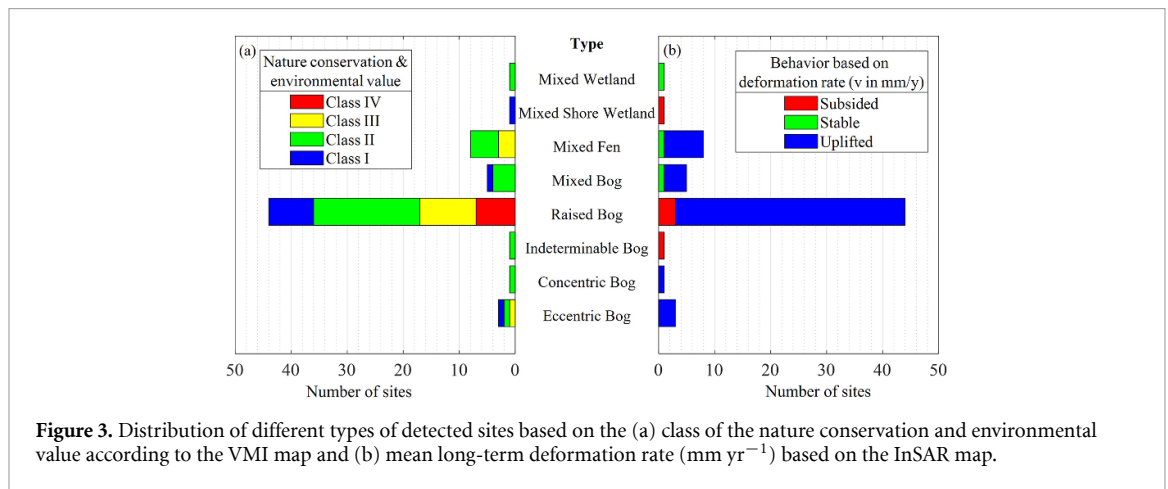


Figure 3. Distribution of different types of detected sites based on the (a) class of the nature conservation and environmental value according to the VMI map and (b) mean long-term deformation rate (mm yr^{-1}) based on the InSAR map.

The abovementioned results show the InSAR technique’s ability to detect the deformation of the bog peatland areas. The efficiency of the InSAR technique decreases commensurately with increasing the amount of woody and massive plants (e.g. trees and shrubs) in the sites because of the reduction of the backscattered SAR signal’s correlation. Most detected peat sites were classified in classes I and II, corresponding to the highest importance regarding nature conservation and environmental value. Furthermore, roughly 86% of all detected sites showed uplift (i.e. positive long-term deformation rate of more than 3 mm yr^{-1}), representing good conditions for peat accumulation. Amongst the detected bog-type peat sites, 91% experienced uplift, as shown in

figure 3. Only 8% of all 64 sites experienced subsidence (table S4). Most of the detected peat sites were of bog type, which highlights the efficacy of InSAR processing in detecting the bog-type peat sites along with their deformation rates.

Six representative sites out of the 64 detected sites were selected to simplify the discussion and provide insight into the results. The selected representative sites covered the whole spectrum of deformation and satisfied the detection criteria regarding the SDFP pixels discussed in section 3. Figure 4(a) shows the distribution of these sites.

The mean TS-InSAR deformation of the six representative peat sites (denoted by a to f) was calculated by averaging the deformation of SDFP pixels

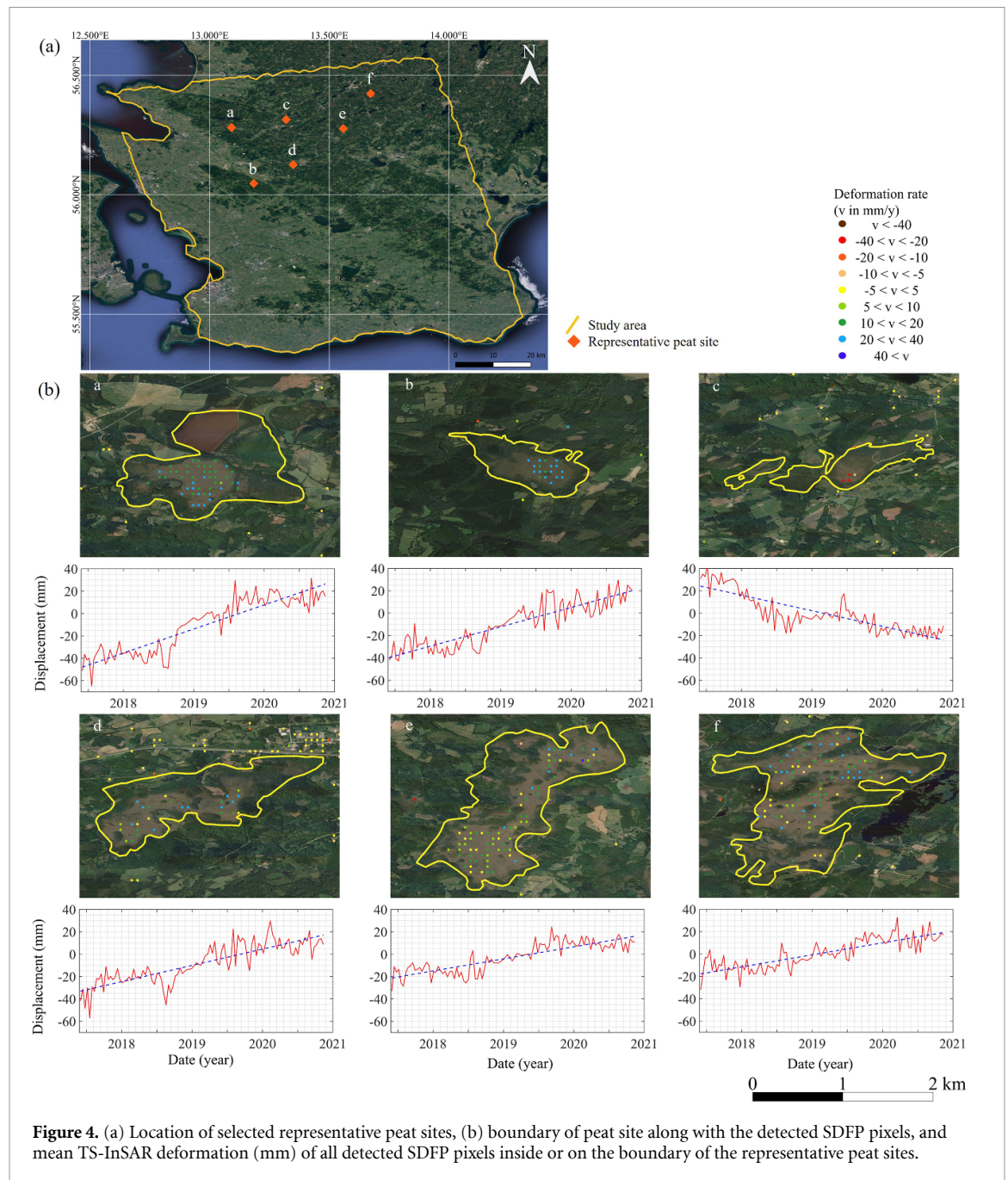


Figure 4. (a) Location of selected representative peat sites, (b) boundary of peat site along with the detected SDFP pixels, and mean TS-InSAR deformation (mm) of all detected SDFP pixels inside or on the boundary of the representative peat sites.

inside each site. The mean TS values for each site over the study period are shown in figure 4(b), along with the locations of the detected SDFP pixels. Figure 4(b) includes the long-term deformation trend at each site, represented by a dashed blue line. The detected trends were positive at five sites (sites a, b, d, e, and f) and only negative at one site (site c).

Despite the expected water table drawdown due to the severe 2018 drought, most of the study sites exhibited an uplift over the 2017–2020 period. It seems that bogs are resistant to climate extremes, as argued by Peregon *et al* (2007), Wu and Roulet (2014), and Salimi *et al* (2021b). Moreover, it seems that in a warmer climate, different types of plants in peatlands might be favored by the altered environmental

conditions and increase their biomass (Heijmans *et al* 2008). Increasing the temperature may favor vascular plant growth (McPartland *et al* 2020, Salimi *et al* 2021b) and expansion, whereas increased CO_2 due to mass plant degradation may benefit *Sphagnum* growth (Heijmans *et al* 2008, Mäkiranta *et al* 2018). In our study, the growing season was warmer and longer than usual in 2018 (Moravec *et al* 2021) and partially in 2019 (figure S4), which could enhance bog photosynthesis and CO_2 uptake for most of the sites, which is confirmed by the mesocosm experiment by Salimi *et al* (2021b).

The possible lower water table caused by a higher evapotranspiration rate during the 2018 drought introduced oxygen to the peat top layers, where the

labile organic matter can rapidly decompose and supply nutrients to the plants. These available nutrients fertilize the plants and boost their photosynthetic capacity (Munir et al 2015, Walker et al 2015, Ratcliffe et al 2019), leading to a higher plant growth rate, carbon accumulation, and consequently, surface uplift. This is especially important for bogs, which have a nutrient-poor environment compared to fen, as evidenced by the findings of this study, where most detected sites included bogs. Furthermore, the warmer growing seasons of 2018 and partially 2019 could have resulted in a shift from the bryophytes to vascular plants, which are fast-growing and less susceptible to drought. This is because their roots can penetrate deeper layers where the water/soil moisture is sufficient for active photosynthesis and carbon sequestration (Weltzin et al 2003, Breeuwer et al 2010, Potvin et al 2015, Mäkiranta et al 2018). It appears that in those few sites where subsidence was observed, the plant shift (from *Sphagnum* dominance to vascular plant dominance) did not occur. *Sphagnum* remained the dominating plant at the site, hence affected by the 2018 drought, which resulted in subsidence. This subsidence may occur for the *Sphagnum*-dominant peatlands as the spongy structure of *Sphagnum* can be damaged during an extreme drought, resulting in a loss of moisture-holding capacity, which leads to *Sphagnum* shrinking and eventually subsidence. Therefore, the behavior of peatland surface motion can be greatly influenced by the dominant plant response to the altered climate conditions, as different plant types may respond to climate change in different ways (Leifeld and Menichetti 2011, Dieleman et al 2015, Leifeld and Menichetti 2018).

4.2. Carbon sequestration

Estimating the annual carbon flux emission and uptake at the 64 detected sites was performed using equation (2), which is discussed in section 3. The calculations showed that the total area of the detected sites is 9198 ha, out of which 14% (1280 ha) were stable or experienced average subsidence of 9 mm yr⁻¹, corresponding to a net carbon emission of 2336 tons yr⁻¹ into the atmosphere.

However, the remaining 86% (7918 ha), with an average uplift of 13 mm yr⁻¹, acted as a carbon sink with 46 972 tons yr⁻¹ of carbon absorption during the 2017–2020 period.

It is worth mentioning that the bulk density and carbon concentration, used in equation (2) to calculate the carbon flux, are related to the type, age, and depth of the accumulated peat. Ideally, these parameters should be measured in the laboratory or on-site, which was impossible in this study. Hence, the abovementioned calculations are an estimation of the carbon flux, and we have assumed all sites

as temperate peatlands with identical properties over their area, as also assumed by Hoyt et al (2020).

The findings of this study indicate that bogs are resilient to warmer and drier conditions and can maintain their sink function and accumulate carbon despite drier and warmer periods (Peregon et al 2007, Wu and Roulet 2014, Salimi et al 2021b). But this may not be the case in the long term as this accumulation could be balanced by a higher decomposition rate of the labile organic matter produced by vascular plants. Continuous monitoring by the InSAR technique can be used to monitor the deformation of peatland ecosystems over a more extended period to improve the understanding of the peatland ecosystem's response to climate variability and change.

5. Conclusion

This study highlights InSAR's ability to detect the deformation rate of peatland areas. The technique could effectively detect vertical displacement over the peatland sites during the 3.5 years. The detected sites were categorized into eight types according to the VMI map, including bog types or mixed types as the main feature. About 89% of all detected sites were categorized as having a high nature conservation and environmental value as they belonged to the first three of four defined categories.

Almost 91% of the detected bog-type peat sites experienced uplift during the study period, notwithstanding the drought of the summer of 2018. These results are corroborated by Salimi et al (2021b), who studied unmanaged mesocosms peats from the studied area.

The calculated deformation map using the InSAR technique was translated into carbon flux to quantify their contribution to climate change mitigation. The results show that most sites act as a sink for carbon by sequestering about 47 kilotons yr⁻¹ despite the 2018 drought.

The methodology developed in this study can be extended to all peatland areas in different climate conditions as a standard and effective method for monitoring carbon sequestration around the globe. Water table data are useful in assessing peat storage changes concerning the hydrological cycle. More specific and accurately measured parameters involved in carbon flux calculation are recommended to improve reliable carbon sequestration results.

Data availability statement

The data cannot be made publicly available upon publication because no suitable repository exists for hosting data in this field of study. The data that support the findings of this study are available upon reasonable request from the authors.

Acknowledgments

This research was funded by the Strategic Research Area: The Middle East in the Contemporary World (MECW) at the Centre for Advanced Middle Eastern Studies, Lund University, Sweden. The authors would like to thank Scripps Institution of Oceanography and San Diego State University for the development of GMTSAR software packages, and the Delft Institute of Earth Observation and Space Systems for the development of the StaMPS/MTI software package, which were used in this work. We would also like to thank the European Space Agency (www.esa.int) for providing Sentinel-1 images and the National Aeronautics Space Administration (NASA) (www.nasa.gov) for providing the SRTM DEM. We also thank the National Land Survey of Sweden (Lantmäteriet), the Swedish Wetlands Inventory (VMI), and Swedish Meteorological and Hydrological Institute (SMHI) for providing the auxiliary and validation data for this work. The computations for this study were partially enabled by resources provided by LUNARC.

ORCID iDs

Behshid Khodaei  <https://orcid.org/0000-0001-7093-7614>

Hossein Hashemi  <https://orcid.org/0000-0003-2160-1772>

References

- Official Statistics of Sweden (SCB) 2020 *Land Use in Sweden* (available at: www.scb.se/en/finding-statistics/statistics-by-subject-area/environment/land-use/land-use-in-sweden/pong/tables-and-graphs/land-use-in-sweden-2020/) (Accessed 10 January 2022)
- Alshammari L, Boyd D S, Sowter A, Marshall C, Andersen R, Gilbert P, Marsh S and Large D J 2020 Use of surface motion characteristics determined by InSAR to assess peatland condition *J. Geophys. Res. Biogeosci.* **125** e2018JG004953
- Alshammari L, Large D J, Boyd D S, Sowter A, Anderson R, Andersen R and Marsh S 2018 Long-term peatland condition assessment via surface motion monitoring using the ISBAS DInSAR technique over the Flow Country, Scotland *Remote Sens.* **10** 1103
- Amani M, Poncos V, Brisco B, Foroughnia F, DeLancey E R and Ranjbar S 2021 InSAR coherence analysis for wetlands in Alberta, Canada using time-series Sentinel-1 data *Remote Sens.* **13** 3315
- Berardino P, Fornaro G, Lanari R and Sansosti E 2002 A new algorithm for surface deformation monitoring based on small baseline differential SAR interferograms *IEEE Trans. Geosci. Remote Sens.* **40** 2375–83
- Breeuwer A, Heijmans M M, Robroek B J and Berendse F 2010 Field simulation of global change: transplanting northern bog mesocosms southward *Ecosystems* **13** 712–26
- Campbell A et al 2009 *Review of the literature on the links between biodiversity and climate change: impacts, adaptation and mitigation* p 124 (available at: www.cbd.int/doc/publications/cbd-ts-42-en.pdf)
- Chen J, Knight R, Zebker H A and Schreuder W A 2016 Confined aquifer head measurements and storage properties in the San Luis Valley, Colorado, from spaceborne InSAR observations *Water Resour. Res.* **52** 3623–36
- Chen Y, Zhang G, Ding X and Li Z 2000 Monitoring earth surface deformations with InSAR technology: principles and some critical issues *J. Geospat. Eng.* **2** 3–22
- Cigna F, Sowter A, Jordan C J and Rawlins B G 2014 Intermittent small baseline subset (ISBAS) monitoring of land covers unfavourable for conventional C-band InSAR: proof-of-concept for peatland environments in North Wales, UK *SPIE 9243, SAR Image Analysis, Modeling, and Techniques XIV* (Amsterdam: International Society for Optics and Photonics) p 924305
- Couwenberg J and Hooijer A 2013 Towards robust subsidence-based soil carbon emission factors for peat soils in South-East Asia, with special reference to oil palm plantations *Mires Peat* **12** 1–13 (available at: <http://mires-and-peat.net/pages/volumes/map12/map1201.php>)
- Dieleman C M, Branfireun B A, McLaughlin J W and Lindo Z 2015 Climate change drives a shift in peatland ecosystem plant community: implications for ecosystem function and stability *Glob. Change Biol.* **21** 388–95
- Dise N B 2009 Peatland response to global change *Science* **326** 810–1
- Dunn C and Freeman C 2011 Peatlands: our greatest source of carbon credits? *Carbon Manage.* **2** 289–301
- Ferretti A, Prati C and Rocca F 2000 Nonlinear subsidence rate estimation using permanent scatterers in differential SAR interferometry *IEEE Trans. Geosci. Remote Sens.* **38** 2202–12
- Franzén L G 2006 Increased decomposition of subsurface peat in Swedish raised bogs: are temperate peatlands still net sinks of carbon *Mires Peat* **1** 1–16
- Fritz C, Campbell D I and Schipper L A 2008 Oscillating peat surface levels in a restiad peatland, New Zealand—magnitude and spatiotemporal variability *Hydrol. Process., Int. J.* **22** 3264–74
- Gorham E 1991 Northern peatlands: role in the carbon cycle and probable responses to climatic warming *Ecol. Appl.* **1** 182–95
- Gunnarsson U and Löfroth M 2014 *The Swedish Wetland Survey: Compiled Excerpts from the National Final Report* (Naturvårdsverket)
- Hedwall P O and Brunet J 2016 Trait variations of ground flora species disentangle the effects of global change and altered land-use in Swedish forests during 20 years *Glob. Change Biol.* **22** 4038–47
- Heijmans M M, Mauquoy D, Van Geel B and Berendse F 2008 Long-term effects of climate change on vegetation and carbon dynamics in peat bogs *J. Veg. Sci.* **19** 307–20
- Holden J, Chapman P J and Labadz J C 2004 Artificial drainage of peatlands: hydrological and hydrochemical process and wetland restoration *Prog. Phys. Geogr.* **28** 95–123
- Hooijer A, Page S, Jauhiainen J, Lee W A, Lu X X, Idris A and Anshari G 2012 Subsidence and carbon loss in drained tropical peatlands *Biogeosciences* **9** 1053–71
- Hooper A 2008 A multi-temporal InSAR method incorporating both persistent scatterer and small baseline approaches *Geophys. Res. Lett.* **35** 1–5
- Hooper A, Segall P and Zebker H 2007 Persistent scatterer interferometric synthetic aperture radar for crustal deformation analysis, with application to Volcán Alcedo, Galápagos *J. Geophys. Res. Solid Earth* **112** 1–21
- Hooper A, Zebker H, Segall P and Kampes B 2004 A new method for measuring deformation on volcanoes and other natural terrains using InSAR persistent scatterers *Geophys. Res. Lett.* **31** 1–5
- Hoyt A M, Chaussard E, Seppäläinen S S and Harvey C F 2020 Widespread subsidence and carbon emissions across Southeast Asian peatlands *Nat. Geosci.* **13** 435–40
- Jaramillo F, Brown I, Castellazzi P, Espinosa L, Guitard A, Hong S H, Rivera-Monroy V H and Wdowinski S 2018 Assessment of hydrologic connectivity in an ungauged wetland with InSAR observations *Environ. Res. Lett.* **13** 024003
- Large D J, Marshall C, Jochmann M, Jensen M, Spiro B F and Olaussen S 2021 Time, hydrologic landscape, and the

- long-term storage of peatland carbon in sedimentary basins *J. Geophys. Res. Earth Surf.* **126** e2020JF00576
- Leifeld J and Menichetti L 2018 The underappreciated potential of peatlands in global climate change mitigation strategies *Nat. Commun.* **9** 1–7
- Leifeld J, Müller M and Fuhrer J 2011 Peatland subsidence and carbon loss from drained temperate fens *Soil Use Manage.* **27** 170–6
- Liu H and Lennartz B 2019 Hydraulic properties of peat soils along a bulk density gradient—a meta study *Hydrol. Process.* **33** 101–14
- Lund M, Christensen T R, Lindroth A and Schubert P 2012 Effects of drought conditions on the carbon dioxide dynamics in a temperate peatland *Environ. Res. Lett.* **7** 045704
- Lundblad M 2015 *Land Use on Organic Soils in Sweden: An Overview on Agriculture, Forest Lands and Land Use Changes on Organic Soils* (Norrköping: Swedish Meteorological and Hydrological Institute)
- Mäkiranta P, Laiho R, Mehtätalo L, Straková P, Sormunen J, Minkinen K, Penttilä T, Fritze H and Tuittila E S 2018 Responses of phenology and biomass production of boreal fens to climate warming under different water-table level regimes *Glob. Change Biol.* **24** 944–56
- Marshall C, Large D J, Athab A, Evers S L, Sowter A, Marsh S and Sjögersten S 2018 Monitoring tropical peat related settlement using ISBAS InSAR, Kuala Lumpur International Airport (KLIA) *Eng. Geol.* **244** 57–65
- Marshall C, Sterk H P, Gilbert P J, Andersen R, Bradley A V, Sowter A, Marsh S and Large D J 2022 Multiscale variability and the comparison of ground and satellite radar based measures of peatland surface motion for peatland monitoring *Remote Sens.* **14** 336
- McPartland M Y, Montgomery R A, Hanson P J, Phillips J R, Kolka R and Palik B 2020 Vascular plant species response to warming and elevated carbon dioxide in a boreal peatland *Environ. Res. Lett.* **15** 124066
- Mohammadimanes F, Salehi B, Mahdianpari M, Brisco B and Motagh M 2018 Wetland water level monitoring using interferometric synthetic aperture radar (InSAR): a review *Can. J. Remote Sens.* **44** 247–62
- Moravec V, Markonis Y, Rakovec O, Svoboda M, Trnka M, Kumar R and Hanel M 2021 Europe under multi-year droughts: how severe was the 2014–2018 drought period? *Environ. Res. Lett.* **16** 034062
- Munir T M, Perkins M, Kaing E and Strack M 2015 Carbon dioxide flux and net primary production of a boreal treed bog: responses to warming and water-table-lowering simulations of climate change *Biogeosciences* **12** 1091–111
- Peregon A, Uchida M and Shibata Y 2007 Sphagnum peatland development at their southern climatic range in West Siberia: trends and peat accumulation patterns *Environ. Res. Lett.* **2** 045014
- Potvin L R, Kane E S, Chimner R A, Kolka R K and Lilleskov E A 2015 Effects of water table position and plant functional group on plant community, aboveground production, and peat properties in a peatland mesocosm experiment (PEATcosm) *Plant Soil* **387** 277–94
- Premke K et al 2016 The importance of landscape diversity for carbon fluxes at the landscape level: small-scale heterogeneity matters *Wiley Interdiscip. Rev. Water* **3** 601–17
- Price J S 2003 Role and character of seasonal peat soil deformation on the hydrology of undisturbed and cutover peatlands *Water Resour. Res.* **39** 1241
- Ratcliffe J L, Campbell D I, Clarkson B R, Wall A M and Schipper L A 2019 Water table fluctuations control CO₂ exchange in wet and dry bogs through different mechanisms *Sci. Total Environ.* **655** 1037–46
- Reeve A S, Glaser P H and Rosenberry D O 2013 Seasonal changes in peatland surface elevation recorded at GPS stations in the Red Lake Peatlands, northern Minnesota, USA *J. Geophys. Res. Biogeosci.* **118** 1616–26
- Reeves J A, Knight R and Zebker H A 2014 An analysis of the uncertainty in InSAR deformation measurements for groundwater applications in agricultural areas *IEEE J. Sel. Top. Appl. Earth Obs. Remote Sens.* **7** 2992–3001
- Salimi S, Almuktar S A and Scholz M 2021a Impact of climate change on wetland ecosystems: a critical review of experimental wetlands *J. Environ. Manage.* **286** 112160
- Salimi S, Berggren M and Scholz M 2021b Response of the peatland carbon dioxide sink function to future climate change scenarios and water level management *Glob. Change Biol.* **27** 5154–68
- Sjörs H 1967 *Nordic Plant Geography* 2nd edn (Stockholm: Scandinavian University Books)
- Smith R G, Hashemi H, Chen J and Knight R 2021 Apportioning deformation among depth intervals in an aquifer system using InSAR and head data *Hydrogeol. J.* **29** 2475–86
- Tong X and Schmidt D 2016 Active movement of the Cascade landslide complex in Washington from a coherence-based InSAR time series method *Remote Sens. Environ.* **186** 405–15
- Umarhadi D A, Avtar R, Widyatmanti W, Johnson B A, Yunus A P, Khedher K M and Singh G 2021 Use of multifrequency (C-band and L-band) SAR data to monitor peat subsidence based on time-series SBAS InSAR technique *Land Degrad. Dev.* **32** 4779–94
- Walker T N, Ward S E, Ostle N J and Bardgett R D 2015 Contrasting growth responses of dominant peatland plants to warming and vegetation composition *Oecologia* **178** 141–51
- Wdowinski S and Hong S H 2015 Wetland InSAR: a review of the technique and applications *Remote Sensing of Wetlands: Applications and Advances* ch 7, pp 137–54 (available at: www.routledge.com/Remote-Sensing-of-Wetlands-Applications-and-Advances/Tiner-Lang-Klemas/p/book/9781482237351)
- Weltzin J F, Bridgman S D, Pastor J, Chen J and Harth C 2003 Potential effects of warming and drying on peatland plant community composition *Glob. Change Biol.* **9** 141–51
- Wu J and Roulet N T 2014 Climate change reduces the capacity of northern peatlands to absorb the atmospheric carbon dioxide: the different responses of bogs and fens *Global Biogeochem. Cycles* **28** 1005–24
- Xie C, Shao Y, Xu J, Wan Z and Fang L 2013 Analysis of ALOS PALSAR InSAR data for mapping water level changes in Yellow River Delta wetlands *Int. J. Remote Sens.* **34** 2047–56
- Zhou Z 2013 The applications of InSAR time series analysis for monitoring long-term surface change in peatlands *PhD Thesis* University of Glasgow p 231
- Zhou Z, Li Z, Waldron S and Tanaka A 2019 InSAR time series analysis of L-band data for understanding tropical peatland degradation and restoration *Remote Sens.* **11** 2592